Polarization observables in η and π production using a polarized target with the Crystal Ball/TAPS at MAMI

Natalie K. Walford' , Manuel Dieterle, Bernd Krusche, Thomas Strub, and Lilian Witthauer

Citation: AIP Conference Proceedings **1735**, 040012 (2016); doi: 10.1063/1.4949416
View online: http://dx.doi.org/10.1063/1.4949416
View Table of Contents: http://aip.scitation.org/toc/apc/1735/1
Published by the American Institute of Physics

Polarization Observables in η and π Production Using a Polarized Target with the Crystal Ball/TAPS at MAMI

Natalie K. Walford[1,a)], Manuel Dieterle[1], Bernd Krusche[1], Thomas Strub[1] and Lilian Witthauer[1]

[1]*Department of Physics, University of Basel, Klingelbergstrasse 82, 4056 Basel, Switzerland*

[a)]natalie.walford@unibas.ch

Abstract. Recent experiments using the Crystal Ball/TAPS setup at the MAMI accelerator in Mainz, Germany, continue to study the properties and the excitation spectrum of the nucleon with meson photoproduction. Electromagnetic excitations of the proton and neutron are essential for understanding their isospin decomposition. The electromagnetic coupling of photons to protons is different than that to neutrons in certain states. Hence, a complete partial wave analysis (PWA) can assist in yielding more information about any reaction, but requires the determination of polarization observables. Polarization observables play a crucial role as they are essential in disentangling the contributing resonant and non-resonant amplitudes, whereas cross section data alone is not sufficient for separating broad overlapping resonances. Preliminary results of polarization observables of η, single, and double π production off a polarized neutron (dButanol) target will be shown with comparison to predictions of recent multipole analyses. These results will greatly increase the world database on pseudoscalar meson production on neutrons.

Introduction

The study of the nucleon and its excitation spectrum has been investigated for many decades now. The nucleon spectrum allows for understanding the dynamics and relevant degrees of freedom within hadrons in the non-perturbative regime of quantum chromodynamics (QCD). Solutions of QCD, which describe the strong force acting between quarks, are only solved at very low and high energies where perturbative methods can be used. At medium energies, non-perturbative approximation models describe the behavior of quarks in nucleons. Meson photoproduction can specifically allow for unique possibilities to investigate these nucleons and their excited states (or resonances). However, many states are overlapping and can not be easily differentiated, and many have been predicted, but not yet observed [1]. Those states that have yet to be observed could be missing due to the fact that they have not been seen experimentally yet or do not exist. Those that have been observed have given insight to the broader picture of nucleon resonances. Since most earlier measurements were done using pion beams, some resonances might couple less strongly to pions and could couple more strongly to more rare channels and have missed detection. Most of the results still arise from experiments on the proton, which does not allow for as much information regarding the isospin structure of the electromagnetic transitions. However, advances in experiments on the neutron will give an integral piece to the understanding of the nucleon spectrum. It is not possible to perform measurements on the free neutron, but a deuterated butanol target has allowed for the possibility to study spin effects with quasi-free neutrons.

Cross section data has long been utilized in order to learn about the nucleon spectrum. However, cross section data alone is not enough to distinguish all states due to the overlapping resonances, but polarization observables can provide insight into the overlapping resonances. The interaction between photon beams and nucleons can be described by four complex amplitudes, which are fully determined when a complete set of measurements is performed. These four complex amplitudes give rise to the cross-section, complemented by polarization observables including beam, target, and recoil asymmetries and combinations of beam-target, beam-recoil, and target-recoil polarization asymmetries. This work specifically concerns the measurements of the following polarization observables: E (longitudinally polarized target), F (transversely polarized target), and T (transversely polarized target), which are associated with a circularly polarized photon beam (E and F observables) or an unpolarized photon beam (T observable).

XVIth International Conference on Hadron Spectroscopy
AIP Conf. Proc. 1735, 040012-1–040012-7; doi: 10.1063/1.4949416
Published by AIP Publishing. 978-0-7354-1389-4/$30.00

The relationship between the cross section and polarization observable E can be written in terms of the helicity of the beam as follows:

$$E = \frac{\sigma_{1/2} - \sigma_{3/2}}{\sigma_{1/2} + \sigma_{3/2}} = \frac{\sigma_{1/2} - \sigma_{3/2}}{2 * \sigma_0},$$

where $\sigma_{1/2}$ is the cross section of events with anti-parallel beam and target polarizations with total spin $\frac{1}{2}$ and $\sigma_{3/2}$ is the cross section of events with parallel beam with total spin of $\frac{3}{2}$.

Additionally, the relationship between the cross section and polarization observable T and F is defined as the following:

$$\frac{d\sigma}{d\Omega} = \frac{1}{2}\frac{d\sigma_0}{d\Omega}(1 + TP_T sin\phi + FP_C P_T cos\phi),$$

where P_T is the transverse polarization of the target and ϕ is the angle between the target spin and the reaction plane.

Experimental Setup

The data described herein is from experiments performed at the MAMI-C accelerator in Mainz, Germany [2]. A longitudinally polarized electron beam of energy 1.557 GeV and polarization degree of 80% is delivered into the A2 Hall. Circularly polarized photons are produced from a radiator foil and energy tagged using the Glasgow-Mainz photon tagger [3] with energies between 0.47 and 1.45 GeV. The target consists of deuterated butanol (D_9C_4OD) cooled to a low temperature with the deuterons either transversally or longitudinally polarized up to 80%. The target is surrounded by a cylindrical particle identification detector (PID) made of 24 plastic scintillator strips that each cover 15° in the azimuthal angle. The PID is then surrounded by a multi-wire proportional chamber (MWPC) and the MWPC is surrounded by the spherical Crystal Ball (CB) calorimeter [4]. The CB consists of 672 NaI(Tl) crystals and covers 20° to 160° in the polar angle. In the forward direction, a hexagonal two arm photon spectrometer (TAPS) built from 72 $PbWO_4$ (inner two rings) and 366 BaF_2 crystals (remaining outer rings) is present. A VETO wall in front of TAPS is used for particle identification. The combination of the CB and TAPS provides an almost 4π acceptance in the center of mass frame with a high angular and energy resolution. An overview of the Crystal Ball/TAPS setup can be seen in Fig. 1.

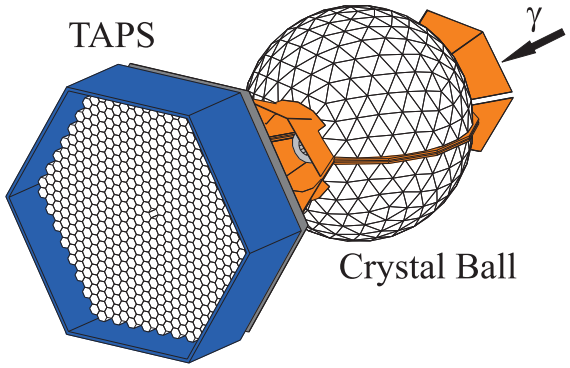

FIGURE 1. Overview of the Crystal Ball/TAPS experiment in A2 at MAMI. The photon beam enters and hits the targets with decay products detected in the Crystal Ball and TAPS detectors.

Analysis and Results

Events were collected and then selected based on the number of charged or neutral hit information desired from the detectors. Neutral mesons are identified via a χ^2 test, which finds the best combination of photon clusters for the meson invariant mass. Coincidence time cuts were applied to eliminate accidentally coincident tagger photons, and a random background subtraction was performed. To separate the background, kinematic cuts were applied for each W

and θ bin. Relevant events come from the polarized deuterons with cuts applied. Using data from a carbon target (^{12}C) beamtime of similar experimental conditions, the subtraction of reactions on unpolarized carbon and oxygen nuclei inside the dButanol target was performed. Further studies of the contribution of reactions on unpolarized nuclei was done by comparing the missing mass spectra of the dButanol, liquid deuterium, and carbon beam times.

TABLE 1. Overview of the versions used to extract the E asymmetry.

Version	E	$\sigma_{1/2}$	$\sigma_{3/2}$
1	$\frac{\sigma_\Delta}{2*\sigma_0}$	$\sigma_0(1 + E)$	$\sigma_0(1 - E)$
2	$\frac{\sigma_\Delta}{\sigma_\Sigma}$	$\sigma_0(1 + E)$	$\sigma_0(1 - E)$
3		$\frac{\sigma_\Sigma+\sigma_\Delta}{2}$	$\frac{\sigma_\Sigma-\sigma_\Delta}{2}$
4	$\frac{\sigma_{1/2}-\sigma_{3/2}}{\sigma_{1/2}+\sigma_{3/2}}$	$\sigma_{1/2}$	$\sigma_{3/2}$

Different versions were used to extract the final E asymmetry in the end. *Version 1* refers to where the asymmetry was normalized with twice the unpolarized cross section σ_0, which was measured with a liquid deuterium target, and does not need to utilize carbon background subtraction since the unpolarized background cancels in the difference of the two helicity states ($\sigma_\Delta = \sigma_{1/2} - \sigma_{3/2}$). *Version 2* refers to the normalization of the numerator using the sum of the two spin configurations ($\sigma_\Sigma = \sigma_{1/2} + \sigma_{3/2}$). Here, the background from unpolarized carbon and oxygen nuclei inside the target have to be subtracted, allowing for events only on polarized protons and neutrons. *Version 3* refers to using the sum and difference of the two helicity states to calculate E and the carbon was used to subtract the unpolarized carbon and oxygen nuclei. Finally, *version 4* refers to using a direct calculation of $\sigma_{1/2}$ and $\sigma_{3/2}$. An overview of the different versions are summarized in Table 1.

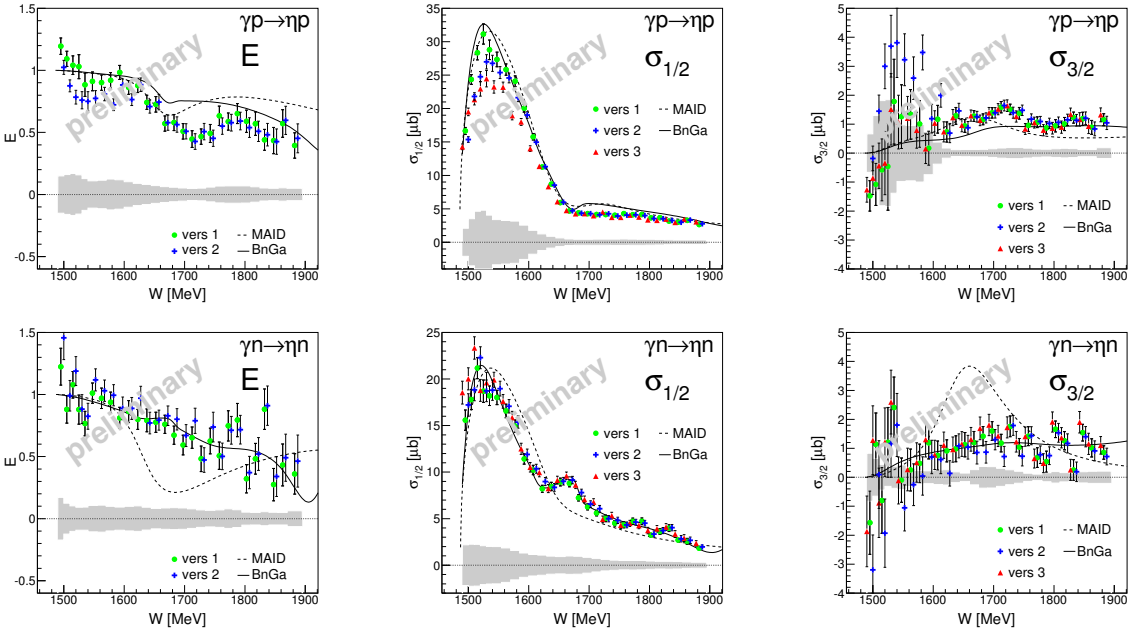

FIGURE 2. E (first column), $\sigma_{1/2}$ (middle column), and $\sigma_{3/2}$ (last column) asymmetries for η for quasi-free protons (upper row) and quasi-free neutrons (lower row). Dashed lines are MAID [5] nucleon models and solid lines are Bonn-Gatchina [6] nucleon models. Results include statistical and systematic (indicated in grey) errors and are preliminary. Green circles refer to data obtained using *version 1*, blue crosses refer to data obtained using *version 2*, and red triangles refer to data obtained using *version 3*.

The E asymmetry for η photoproduction can be seen in Fig. 2. E is roughly one close to threshold for both protons and neutrons, as seen in the first column. In the last column, it can be seen that for both proton and neutrons, the contributions from $\sigma_{3/2}$ is small. However, the contribution from $\sigma_{1/2}$ for neutrons is clearly visible in the middle

column as a bump-like structure occuring around $W = 1670$ MeV, which is not present in the proton data. The Bonn-Gatchina model explains the bump due to an interference of the spin-$\frac{1}{2}$ N(1535) and N(1650) resonances.

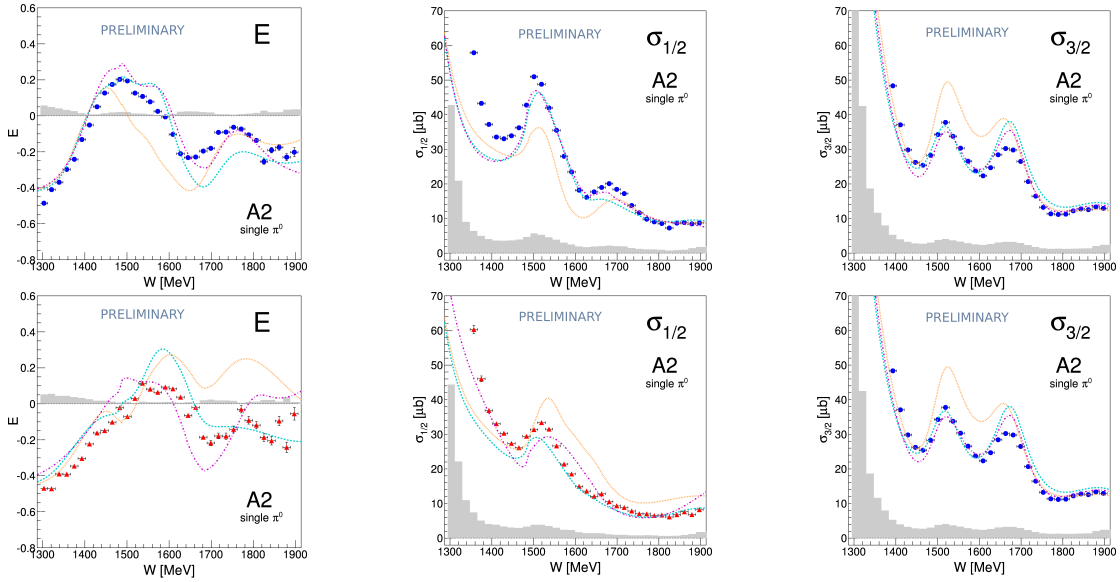

FIGURE 3. E (first column), $\sigma_{1/2}$ (middle column), and $\sigma_{3/2}$ (last column) asymmetries for single π^0 for quasi-free protons (upper row) and quasi-free neutrons (lower row). The cyan lines are SAID [7] nucleon models, the orange lines are MAID [5] nucleon models, and the magenta lines are Bonn-Gatchina [8][9] nucleon models. Open triangles refer to data obtained using *version 1*, open diamonds refers to data obtained using *version 2*, open circle refers to data obtained using *version 3*, and open squares refers to data obtained using *version 4*. Results include statistical and systematic (indicated in grey bars) errors and are preliminary.

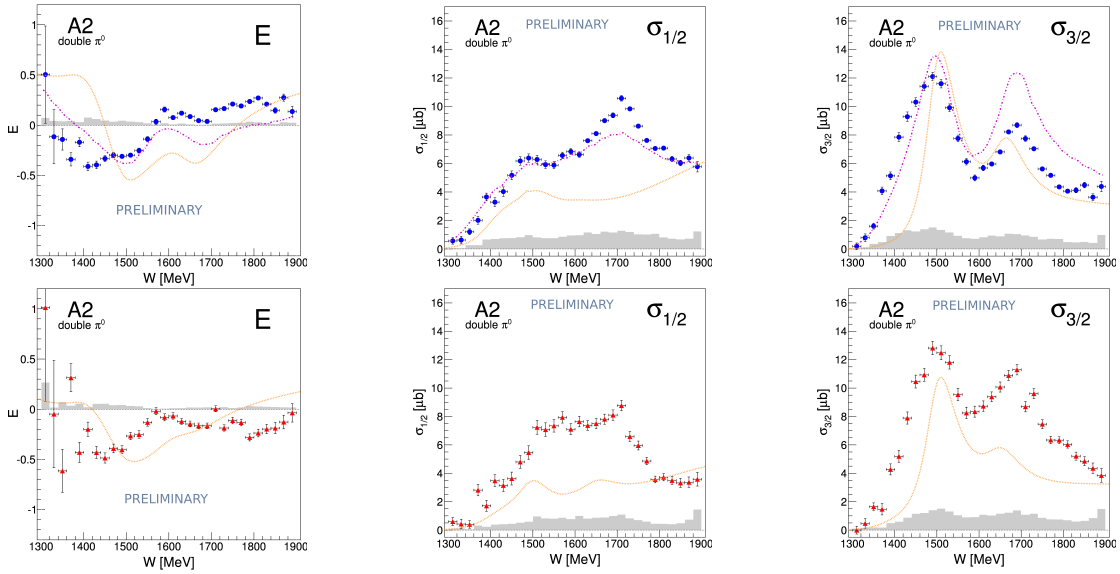

FIGURE 4. E (first column), $\sigma_{1/2}$ (middle column), and $\sigma_{3/2}$ (last column) asymmetries for double π^0 for quasi-free protons (upper row) and quasi-free neutrons (lower row). The orange lines are MAID [10] nucleon models and the magenta lines are Bonn-Gatchina [9] nucleon models. Open triangles refers to data obtained using *version 1*, open diamonds refers to data obtained using *version 2*, open circle refers to data obtained using *version 3*, and open squares refers to data obtained using *version 4*. Results include statistical and systematic (indicated in grey bars) errors and are preliminary.

The E asymmetry for single π^0 photoproduction can be seen in Fig. 3. For single π^0 photoproduction off the

proton, the models do not match the data, but have a similar trend with the bump-like structures occurring around $W = 1500$ MeV and 1680 MeV in $\sigma_{1/2}$ and $W = 1540$ and 1660 MeV in $\sigma_{3/2}$. However, for the neutron data, the models differ more than for the proton. It appears that for lower energies (< 1500 MeV) in E, the models agree, but at higher energies, all models diverge. The SAID model appears to match the data best for both $\sigma_{1/2}$ and $\sigma_{3/2}$.

The E asymmetry for double π^0 photoproduction can be seen in Fig. 4. Here it can be seen that the different versions are in good agreement with each other. The models do not agree with the data at any energy, but appear to have a similar structure as the data in $\sigma_{3/2}$, but not in the $\sigma_{1/2}$. Also, Bonn-Gatchina has no neutron model for double π^0 photoproduction.

The T and F asymmetries were extracted using two opposite spin states for both the photon helicity and the nucleon spin. A dilution factor accounts for the bound nuclei contribution. The T and F asymmetries for η photoproduction can be seen in Fig. 5. Only one of the six measured cos θ bins is shown. It is seen here that the asymmetries for free and quasi-free protons are in good agreement. However, there are significant deviations between the models and the data at all energies.

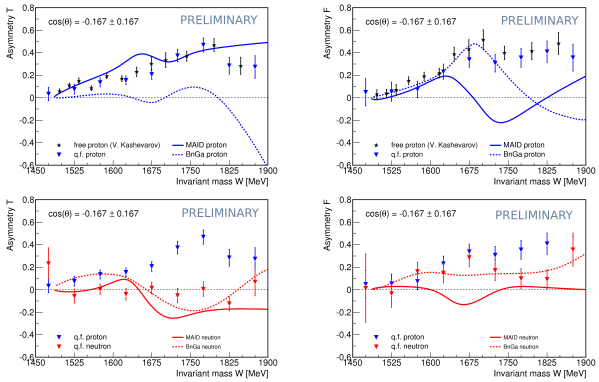

FIGURE 5. T and F asymmetries for η for protons and neutrons measured with a transversely polarized target. Solid lines are MAID nucleon models and dashed lines are Bonn-Gatchina nucleon models with blue referring to proton and red referring to neutron. Blue and red diamonds are data from quasi-free protons and neutrons. Black stars are preliminary data from V. Kashevarov on quasi-free protons. Results include statistical errors only and are preliminary.

One cos θ bin out of the measured 15 bins is shown from T and F asymmetries for single π^0 photoproduction and can be seen in Fig. 6. Here, it is clear that the asymmetries for free and quasi-free protons agree. However, significant deviations between PWA models and the data occur. This is due to the lack of experimental data available, and with this data the models can be improved.

T and F asymmetries for double π^0 photoproduction can be seen in Fig. 7. Here, only one out of eight measured bins is shown. In these figures, the quasi-free and free proton asymmetries agree, but most interestingly is that the proton and neutron asymmetries are very similar.

In conclusion, it is clear that measurements with coincident neutrons in neutral final states are necessary for the analysis of N^* properties. The results from MAMI range in energies never detected before, and due to the lack of neutron data in the world database, these results will provide answers in constraining the current PWA models and help to extract undiscovered states of the nucleon.

Acknowledgments

All results presented in this paper have been obtained in the framework of the A2 collaboration at the Mainz MAMI accelerator. This work was supported by Swiss National Fund (SNF) and Deutsche Forschungsgemeinschaft (DFG).

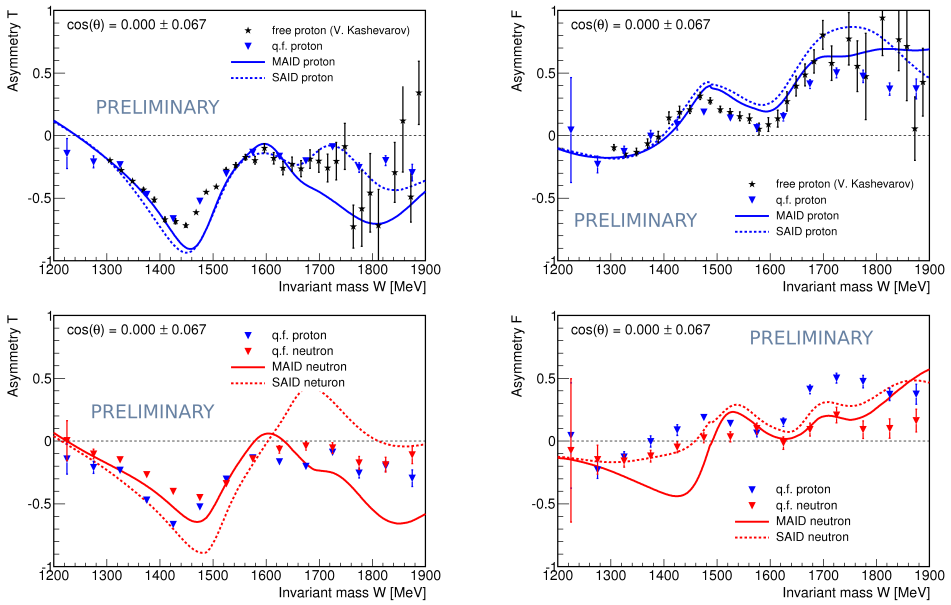

FIGURE 6. T and F asymmetries for single π^0 for protons and neutrons measured with a transversely polarized target. Solid blue and red lines are MAID nucleon models and dashed blue and red lines are SAID nucleon models. Results include statistical errors only and are preliminary.

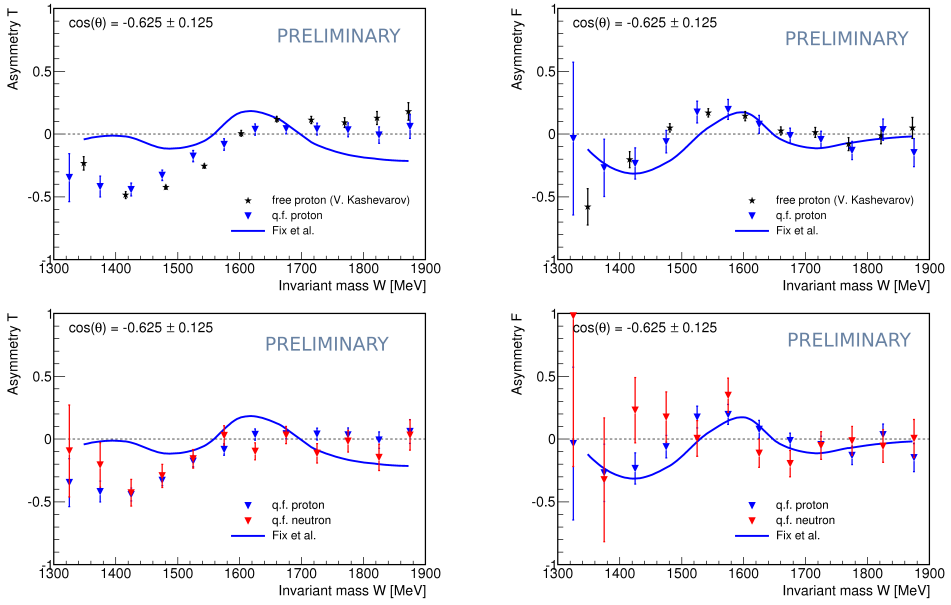

FIGURE 7. T and F asymmetries for double π^0 for protons and neutrons measured with a transversely polarized target. Solid blue lines are MAID [10] Fix nucleon models. Results include statistical errors only and are preliminary.

REFERENCES

[1] R.G. Edwards *et al*., Phys. Rev. **D84** (2011) 074508.
[2] K. H. Kaiser *et al*., NIM **A593** (2008) 159.
[3] J. C. George *et al*., Eur. Phys. J. **A37** (2008) 129.
[4] A. Starostin *et al*., Phys. Rev. **C64** (2001) 055205.
[5] W.-T. Chiang *et al*., Nucl. Phys. **A700** (2002) 429.
[6] A. V. Anisovich *et al*., Eur. Phys. J. **A50** (2014) 74.
[7] R.L. Workman, M. Paris, W.J. Briscoe, I.I. Strakovsky, Phys. Rev. **C86** (2012) 015202.
[8] A. V. Anisovich *et al.*, Eur. Phys. J. **A48** (2011) 15.
[9] E. Gutz *et al*., Eur. Phys. J. **A50** (2014) 74.
[10] H. Arenhoevel and A. Fix, Eur. Phys. J. **A25** (2005) 115.